SCIENCE CHINA
Information Sciences

Modeling and adaptive control for a spatial flexible spacecraft with unknown actuator failures

Zhijie LIU[1,2], Zhiji HAN[1], Zhijia ZHAO[3] and Wei HE[1,*]

Citation: SCIENCE CHINA Information Sciences **64**, 152208 (2021); doi: 10.1007/s11432-020-3109-x

View online: https://engine.scichina.com/doi/10.1007/s11432-020-3109-x

View Table of Contents: https://engine.scichina.com/publisher/scp/journal/SCIS/64/5

Published by the Science China Press

SCIENCE CHINA
Information Sciences

• RESEARCH PAPER •

May 2021, Vol. 64 152208:1–152208:16
https://doi.org/10.1007/s11432-020-3109-x

Modeling and adaptive control for a spatial flexible spacecraft with unknown actuator failures

Zhijie LIU[1,2], Zhiji HAN[1], Zhijia ZHAO[3] & Wei HE[1*]

[1]*Key Laboratory of Knowledge Automation for Industrial Processes of Ministry of Education, School of Automation and Electrical Engineering, Institute of Artificial Intelligence, University of Science and Technology Beijing, Beijing* 100083*, China;*
[2]*Shunde Graduate School of University of Science and Technology Beijing, Foshan* 528300*, China;*
[3]*School of Mechanical and Electrical Engineering, Guangzhou University, Guangzhou* 510006*, China*

Received 10 July 2020/Revised 4 August 2020/Accepted 1 September 2020/Published online 8 April 2021

Abstract In this paper, we address simultaneous control of a flexible spacecraft's attitude and vibrations in a three-dimensional space under input disturbances and unknown actuator failures. Using Hamilton's principle, the system dynamics is modeled as an infinite dimensional system captured using partial differential equations. Moreover, a novel adaptive fault tolerant control strategy is developed to suppress the vibrations of the flexible panel in the course of the attitude stabilization. To determine whether the system energies, angular velocities and transverse deflections, remain bounded and asymptotically decay to zero in the case wherein the number of actuator failures is infinite, a Lyapunov-based stability analysis is conducted. Finally, extensive numerical simulations are performed to demonstrate the performance of the proposed adaptive control strategy.

Keywords adaptive control, actuator failures, infinite-dimensional systems, flexible spacecraft, fault tolerant control

Citation Liu Z J, Han Z J, Zhao Z J, et al. Modeling and adaptive control for a spatial flexible spacecraft with unknown actuator failures. Sci China Inf Sci, 2021, 64(5): 152208, https://doi.org/10.1007/s11432-020-3109-x

1 Introduction

Owing to their advantages such as light weight and low power consumption, flexible structures are applied to modern spacecraft to achieve an increased functionality at a reduced launch cost. Such features can significantly degrade the performance of spacecraft through the introduction of undesired coupling between transverse defections and attitude dynamics. Therefore, the active control of the attitude and the vibrations of flexible spacecraft has become a topic of primary interest. Moreover, several control technologies have been reported in the literature [1–4]. However, the above-mentioned attitude and vibration control schemes of flexible spacecraft are designed based on the truncation approximation models, which suffer from spillovers and even cause instability of the systems. Therefore, to avoid such situations, the flexible spacecraft can be modeled more accurately using an infinite dimensional system of coupled partial differential equations (PDEs) and ordinary differential equations (ODEs) [5–9].

In recent decades, the control problems of flexible structures described by infinite dimensional systems have received considerable attention. Several control schemes have been developed for heat equations [10, 11], beam equations [12–14], string equations [15–18], and other common equations employed in flexible systems. In particular, flexible spacecraft are generally described using Euler-Bernoulli beam models. In [9], the flexible spacecraft is modeled as a flexible cantilever beam to which a rigid hub is attached. Moreover, the vibration reduction and attitude control under external disturbances are addressed through the utilization of disturbance observer-based control schemes. To reduce the vibrations of both flexible panels in [6], which are installed on the central body of the flexible spacecraft comprising a rigid hub with two flexible solar panels, disparate controllers are employed. However, all these studies address

* Corresponding author (email: weihe@ieee.org)

the dynamic analysis, vibration reduction, and attitude regulation of flexible spacecraft in a restricted two-dimensional (2D) plane. The dynamics and control design in a three-dimensional (3D) space are more complicated compared with the modeling and control problems in the 2D plane. With regard to the flexible system operation in a 3D space, such modeling and control problems of flexible beams and risers are relevant to this study. Several studies have investigated the modeling and control design of beams and risers in a 3D space, and boundary control schemes to suppress vibrations have been proposed in [19,20]. However, these studies only resolve the problem on vibration suppression of the beam or riser, without involving the position or attitude control. The strong couplings of displacements in the Y_b and Z_b directions, and the couplings in displacements and the attitude (see Section 2), need to be considered. Moreover, most studies only deal with the vibration control, with assumption that no actuator faults or failures exist. For the flexible spacecraft described by coupled PDEs and ODEs, the coupled mechanical characteristics make it extremely difficult to design control laws and conduct stability analysis, especially in the case of input disturbances and infinite number of actuator failures.

Owing to abrasion, aging, and manufacturing defect, actuators may experience failures during practical operation. Faults on actuators may occur at unknown time instants with unknown values and patterns, which result in the loss of system control or even catastrophic accidents. To guarantee good reliability and safe operation of flexible spacecraft, actuator faults or failures during the entire attitude maneuvers should be considered. In addition, a great deal of achievement has been made through the employment of varieties of active approaches such as robust control, sliding mode control, adaptive control and other methods [21–26]. Especially for flexible spacecraft, numerous measures have been taken to deal with actuator failures [27–30]. In [27,31], a fault-tolerant control method for the flexible spacecraft is proposed to deal with the partial loss of actuator effectiveness. For total loss of control failure, an observer-based fault detection and diagnosis scheme, combined with the sliding mode control technology, is reported to have the ability to control the attitude of a satellite under actuator faults in [28]. In [29], a fault-tolerant control method using quaternion and angular velocity feedback is proposed to deal with actuator failures. Moreover, in [30], a fault-tolerant fuzzy switching control scheme is developed for the attitude stabilization of the flexible spacecraft with stochastic failures. These algorithms are not necessary to obtain the detailed information of actuator failures with the fault detection part. However, these fault-tolerant control schemes for flexible spacecraft are designed based on the truncation approximation models, which may be ineffective in a PDE-based system. To reduce the undesirable influence of the failed actuators, adaptive methods and the Nussbaum gain technique are generally employed to deal with the problem on actuator fault-tolerant control of PDE-based systems [32,33]. Though effectively addressing actuator failures, these methods fail to tackle countless failures and redundant actuators. The actuator failures considered in [32] are offset using adaptive methods but limited to some constants for both actuator efficiency factors and stuck faults. The Nussbaum gain technique is capable of handling a time-varying actuator fault; however, it may not be feasible for redundant actuators. Considering all these studies, the challenge for our study is the simultaneous suppression of the vibrations of the flexible panel and stabilization of the attitude of the spacecraft that is subject possibly to countless unknown actuator failures.

The research object of this paper is the consideration of the simultaneous control problem of the attitude and deflections of the flexible spacecraft in a 3D space. An adaptive boundary control scheme is designed based on the PDEs to stabilize the flexible spacecraft which is subject possibly to an infinite number of unknown actuator failures. Adaptive boundary control of PDEs is a well-established field for parabolic PDEs, including heat equations [34,35], and hyperbolic PDEs, including wave equations [36]. The aforementioned studies only focus on a single second-order PDE describing vibrations in one direction. Adaptive control laws have recently been proposed in [37] for the stabilization of a 2×2 one-order linear hyperbolic system. However, the adaptive control of 2D Euler-Bernoulli beam vibrations is limited. Moreover, there are challenges in the design of adaptive boundary control of the flexible spacecraft described by the generalized Euler-Bernoulli beams due to the existence of strong couplings and actuator failures.

In this study, an adaptive fault-tolerant control strategy with parameter update laws is developed through a Lyapunov-based analysis to simultaneously control the attitude and suppress the vibrations under unknown input disturbances and a possibly infinite number of unknown actuator failures. The major contributions of the paper include the following:

(1) A new coupled model of the flexible spacecraft (which consists of a rigid body captured by an ODE and the flexible panel described by two PDEs) is developed. The extended Hamilton principle is

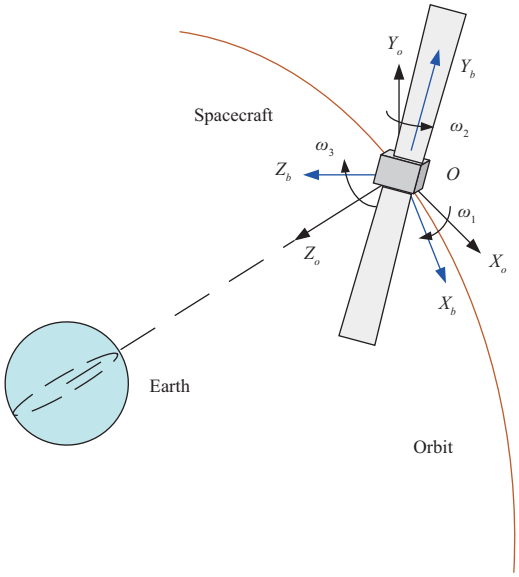

Figure 1 (Color online) Definition of the coordinate systems in the flexible spacecraft fault-tolerant control.

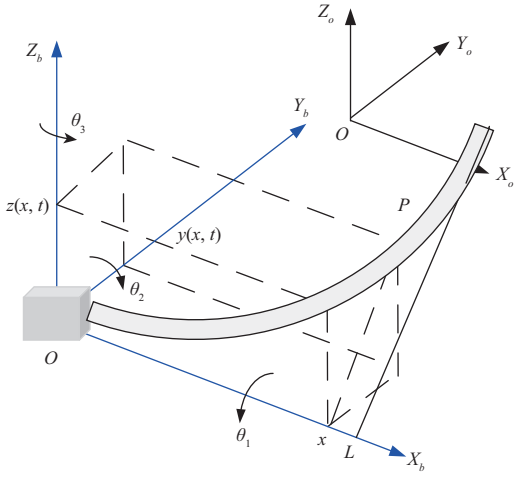

Figure 2 (Color online) Diagram of a 3D flexible spacecraft.

employed to obtain the dynamic model of the coupled system, which considers both the attitude of the spacecraft and vibrations of the flexible panel.

(2) An adaptive control scheme for an unknown failure compensation is reported to simultaneously stabilize the attitude and suppress the vibrations of the flexible spacecraft under the condition that actuators are allowed to switch between normal states and different types of failures for countless times.

(3) The proposed adaptive fault-tolerant control scheme ensures the asymptotic stability of the actuated system; i.e., the attitude and deflections of the flexible spacecraft tend to zero. In addition, the proposed control design is developed based on the Lyapunov direct method, which is easy to grasp and to be applied to other flexible mechanical systems under unknown actuator failures.

The remainder of this paper is organized as follows. In Section 2, the dynamics of a spatial flexible spacecraft described by PDEs coupled with ODEs is presented. A fault-tolerant control scheme and the parameter update laws are described in Section 3. Then, in Section 4, a Lyapunov-based analysis is conducted to evaluate the system energies, angular velocities, and deflections along the Y_b and Z_b axes, which asymptotically decay to zeros. Numerical simulations are described in Section 5 to demonstrate the effectiveness of both methods. Finally, Section 6 concludes the paper.

2 Problem formulation

We consider a typical flexible spacecraft consisting of a rigid body and a slender flexible panel as depicted in Figures 1 and 2. The flexible spacecraft moves in geostationary Earth orbit, and the acceleration of the Earth is assumed to be neglected. We firstly introduce an orbital frame $OX_oY_oZ_o$, with the origin O shared with the body fixed frame $OX_bY_bZ_b$, the axis OX_o tangent to the direction of the orbit, the axis OY_o normal to the orbital plane, and the axis OZ_o pointing to the center of the Earth. We suppose that the undeformed panel is along the OX_b axis, and the panel is inextensible (i.e., we merely consider displacements of the flexible panel in the OY_b and OZ_b directions). Let $y = y(x,t)$ and $z = z(x,t)$ be deflections in OY_b and OZ_b, respectively. Then, the position vector r of the point P on the panel is given by

$$r = [x\ y\ z]^{\mathrm{T}}, \tag{1}$$

where x is the distance measured from the origin O. x and t represent the independent spatial and temporal variables, respectively. $\omega = [\omega_1\ \omega_2\ \omega_3]^{\mathrm{T}}$ describes the angular velocities of the body-fixed frame with respect to the orbital frame. The attitude of the flexible spacecraft is described by Euler angles $\theta = [\theta_1\ \theta_2\ \theta_3]^{\mathrm{T}}$, which are defined as a rotation about X_b, Y_b, and Z_b, respectively.

2.1 Dynamics analysis

In this paper, we assume that the spacecraft is maintained at the desired geosynchronous orbit with suitable control, and only consider the following two types of motions: (1) rotational motion of the rigid hub that changes the orientation of the flexible satellite, and (2) deformation of the flexible panel caused by vibrations.

To develop the dynamical model of the flexible system, we firstly introduce the expression of kinetic energy E_k,

$$E_k = \frac{1}{2}\omega^{\mathrm{T}} I_s \omega + \frac{1}{2}\rho \int_{\Omega} \left[\frac{\mathrm{d}r}{\mathrm{d}t}\right]^{\mathrm{T}} \frac{\mathrm{d}r}{\mathrm{d}t}\mathrm{d}x, \tag{2}$$

where I_s is the inertia tensor of the rigid body and is positive definite and not necessarily diagonal, ρ is the uniformly linear mass of the panel, $\Omega = [0, L]$ with L defined as the length of the flexible panel, and $r = s_0 + s$. The position of P without deformation and with deformation relative to the body frame are denoted by $s_0 = (x, 0, 0)$ and $s = (0, y, z)$, respectively. The time rate of r relative to the orbital frame $OX_oY_oZ_o$ and the body fixed frame $OX_bY_bZ_b$ are $\mathrm{d}r/\mathrm{d}t$ and $\dot{r}$, respectively. We then can obtain

$$\frac{\mathrm{d}r}{\mathrm{d}t} = \dot{r} + \omega \times r = \dot{s} + \omega \times r. \tag{3}$$

We neglect the gravitational energy of the considered system. Then the potential energy generated by deformation of the panel is given by

$$E_p = \frac{1}{2}\int_{\Omega} \left[EI_y y_{xx}^2(x,t) + EI_z z_{xx}^2(x,t)\right] \mathrm{d}x, \tag{4}$$

where EI_y and EI_z are the bending stiffness of the panel for deflections in OY_b axis and OZ_b axis, respectively.

The virtual work δW is calculated by

$$\delta W = (\tau + d)^{\mathrm{T}} \delta\theta - \gamma_b \int_{\Omega} \left[\frac{\mathrm{d}r}{\mathrm{d}t}\right]^{\mathrm{T}} \delta r \mathrm{d}x, \tag{5}$$

where $d = [d_1\ d_2\ d_3]^{\mathrm{T}} \in \mathbb{R}^3$ is input disturbance, $\tau = [\tau_1\ \tau_2\ \tau_3]^{\mathrm{T}} \in \mathbb{R}^3$ is the control torque, and γ_b is the damping coefficient of the panel.

Based on the small deflection property of the panel, Hamilton's principle is utilized to grasp the equations of motion and is expressed by

$$\int_{t_1}^{t_2} (\delta E_k - \delta E_p + \delta W)\, \mathrm{d}t = 0, \tag{6}$$

where δ is the variational operator.

Notice that the virtual displacement δr and the virtual rate $\delta(\mathrm{d}r/\mathrm{d}t)$ of the panel relative to the orbital frame are represented as

$$\delta r = \delta\theta \times r + \delta s, \tag{7}$$

$$\delta(\mathrm{d}r/\mathrm{d}t) = \delta\omega \times r + \delta\theta \times (\omega \times r + \dot{s}) + (\mathrm{d}/\mathrm{d}t)(\delta s), \tag{8}$$

where the virtual rotation rate of the body frame $\delta\omega$ is given as follows:

$$\delta\omega = (\mathrm{d}/\mathrm{d}t)(\delta\theta). \tag{9}$$

The vibrations of (2) and (4) are

$$\begin{aligned}\int_{t_1}^{t_2} \delta E_k \mathrm{d}t &= \int_{t_1}^{t_2} \delta\omega^{\mathrm{T}} (I_s\omega)\, \mathrm{d}t + \rho \int_{t_1}^{t_2}\int_{\Omega} \delta \left[\frac{\mathrm{d}r}{\mathrm{d}t}\right]^{\mathrm{T}} \frac{\mathrm{d}r}{\mathrm{d}t}\mathrm{d}x\mathrm{d}t \\ &= -\int_{t_1}^{t_2}\int_{\Omega} (\mathrm{d}/\mathrm{d}t)(r \times \dot{s})^{\mathrm{T}} \delta\theta \mathrm{d}x\mathrm{d}t - \rho \int_{t_1}^{t_2}\int_{\Omega} (\ddot{s} + \varpi)^{\mathrm{T}} \delta s \mathrm{d}x\mathrm{d}t\end{aligned}$$

$$-\int_{t_1}^{t_2}(\dot{I}_b\omega+I_t\dot{\omega}+\omega\times(I_t\omega))^{\mathrm{T}}\delta\theta\mathrm{d}t, \tag{10}$$

in which $\varpi=2\omega\times\dot{s}+\dot{\omega}\times r+\omega\times(\omega\times r)$, and $I_t=I_s+I_b$. I_t represents the total inertia tensor of the rigid body with respect to the body axes and I_b denotes the panel inertia tensor with respect to the body frame, with definitions

$$I_b=\begin{bmatrix}I_{xx}&-I_{xy}&-I_{xz}\\-I_{xy}&I_{yy}&-I_{yz}\\-I_{xz}&-I_{yz}&I_{zz}\end{bmatrix}, \tag{11}$$

and

$$I_{xx}=\rho\int_\Omega\left(y^2+z^2\right)\mathrm{d}x,\quad I_{xy}=\rho\int_\Omega xy\mathrm{d}x,\quad I_{yy}=\rho\int_\Omega\left(x^2+z^2\right)\mathrm{d}x,\quad I_{xz}=\rho\int_\Omega xz\mathrm{d}x,$$
$$I_{zz}=\rho\int_\Omega\left(x^2+y^2\right)\mathrm{d}x,\quad I_{yz}=\rho\int_\Omega yz\mathrm{d}x.$$

Based on the assumption that the flexible panel is inextensible and considering (4), we can obtain

$$\begin{aligned}\delta E_p=&EI_y\frac{\partial^2y}{\partial x^2}\frac{\partial}{\partial x}\delta y|_0^L-EI_y\frac{\partial^3y}{\partial x^3}\delta y|_0^L+EI_y\int_\Omega\frac{\partial^4y}{\partial x^4}\delta y\mathrm{d}x\\&+EI_z\frac{\partial^2z}{\partial x^2}\frac{\partial}{\partial x}\delta z|_0^L-EI_z\frac{\partial^3z}{\partial x^3}\delta z|_0^L+EI_z\int_\Omega\frac{\partial^4z}{\partial x^4}\delta z\mathrm{d}x.\end{aligned} \tag{12}$$

In view of (7), (5) can be processed further as

$$\delta W=(\tau+d)^{\mathrm{T}}\delta\theta-\gamma_b\int_\Omega\left[r\times\frac{\mathrm{d}r}{\mathrm{d}t}\right]^{\mathrm{T}}\delta\theta\mathrm{d}x-\gamma_b\int_\Omega\left[\frac{\mathrm{d}r}{\mathrm{d}t}\right]^{\mathrm{T}}\delta s\mathrm{d}x. \tag{13}$$

Considering the fact that the variations $\delta\theta_1$, $\delta\theta_2$, $\delta\theta_3$, δy, and δz are arbitrary, we obtain the coupled governing equations of the flexible spacecraft as

$$I_s\dot{\omega}+\omega\times(I_s\omega)+\mu=\tau+d, \tag{14}$$

$$\rho\begin{bmatrix}y_{tt}\\z_{tt}\end{bmatrix}+\gamma_b\left\{\begin{bmatrix}y_t\\z_t\end{bmatrix}+\begin{bmatrix}0&-\omega_1\\\omega_1&0\end{bmatrix}\begin{bmatrix}y\\z\end{bmatrix}+\begin{bmatrix}\omega_3\\-\omega_2\end{bmatrix}x\right\}+\rho\phi\varpi+\begin{bmatrix}EI_yy_{xxxx}\\EI_zz_{xxxx}\end{bmatrix}=0, \tag{15}$$

and the boundary conditions of the PDE-based equations as

$$y(0,t)=z(0,t)=0,\ y_x(0,t)=z_x(0,t)=0,\ y_{xx}(L,t)=z_{xx}(L,t)=0,\ y_{xxx}(L,t)=z_{xxx}(L,t)=0, \tag{16}$$

where μ, ϕ, and ϖ are defined by

$$\mu=[0\ EI_zz_{xx}(0,t)\ -EI_yy_{xx}(0,t)]^{\mathrm{T}},\ \phi=\begin{bmatrix}0&1&0\\0&0&1\end{bmatrix}, \tag{17}$$

$$\varpi=2\begin{bmatrix}0&-\omega_3&\omega_2\\\omega_3&0&-\omega_1\\-\omega_2&\omega_1&0\end{bmatrix}\begin{bmatrix}0\\y_t\\z_t\end{bmatrix}+\begin{bmatrix}-\left(\omega_2^2+\omega_3^2\right)&\omega_1\omega_2-\dot{\omega}_3&\omega_1\omega_3+\dot{\omega}_2\\\omega_1\omega_2+\dot{\omega}_3&-\left(\omega_1^2+\omega_3^2\right)&\omega_2\omega_3-\dot{\omega}_1\\\omega_1\omega_3-\dot{\omega}_2&\omega_2\omega_3+\dot{\omega}_1&-\left(\omega_1^2+\omega_2^2\right)\end{bmatrix}\begin{bmatrix}0\\y\\z\end{bmatrix}+\begin{bmatrix}0\\\omega_1\omega_2+\dot{\omega}_3\\\omega_1\omega_3-\dot{\omega}_2\end{bmatrix}x. \tag{18}$$

Remark 1. The equations of the motion of the spacecraft are described by a combination of PDEs and ODEs. The PDEs (15) and the boundary conditions (16) indicate the dynamics of the flexible panel, whereas (14) represents the attitude dynamics of the rigid hub.

When the deflections of the panel are zero, i.e., $\mu=0$, (14) can be expressed as a well-known dynamics model of a rigid spacecraft [27]. Also (14)–(16) can reduce to the common equations for a 2D flexible spacecraft [9], if the coupling of the deflections along Y_b and Z_b axes is not considered, i.e., the motion of the flexible spacecraft is restricted to a 2D space.

Remark 2. In this study, we just consider the matched disturbance in order to simplify the control design. When the disturbance or uncertainty appears at the uncontrolled end or the governing equations, the control scheme can be designed based on PDE backstepping methods [38, 39].

2.2 Problem formulation

For a flexible spacecraft, thruster and reaction wheels are used for attitude control where failures may occur in drive motor, bearing, or electronics.

To ensure reliable and safe operation, redundant actuators are mounted on the flexible spacecraft, which are defined by

$$\tau_i = \sum_{j=1}^{m_i} \varrho_{i,j} u_{i,j}, \tag{19}$$

where $\varrho_{i,j} \in \mathbb{R}$ is a constant with unknown value yet known direction (the symbol of $\varrho_{i,j}$ is known but the specific value of it is unavailable), indicating the effect of specific actuator torque $u_{i,j}$, and $u_i = [u_{i,1}\ u_{i,2}\ \dots\ u_{i,m_i}]^{\mathrm{T}} \in \mathbb{R}^{m_i}$ is the actual torque generated by all the mounted actuators for $j = 1, 2, \dots, m_i$, $i = 1, 2, 3$.

We then consider the typical actuator failures:

$$u_{i,j}(t) = \sigma_{i,j}(t) v_{i,j}(t) + \overline{u}_{i,j}(t), \tag{20}$$

where

$$\sigma_{i,j}(t) = \begin{cases} \sigma_{i,j,h}, & \text{if } t \in [T^s_{i,j,h}, T^e_{i,j,h}), \\ 1, & \text{if } t \in [T^e_{i,j,h}, T^s_{i,j,h+1}), \end{cases} \quad \overline{u}_{i,j}(t) = \begin{cases} \overline{u}_{i,j,h}, & \text{if } t \in [T^s_{i,j,h}, T^e_{i,j,h}), \\ 0, & \text{if } t \in [T^e_{i,j,h}, T^s_{i,j,h+1}), \end{cases} \tag{21}$$

$$\sigma_{i,j,h} \overline{u}_{i,j,h} = 0. \tag{22}$$

$v_{i,j}(t)$ and $u_{i,j}(t)$ represent the input and output signals of the (i,j)th ($i = 1,2,3; j = 1,2,\dots,m_i$) actuator, respectively. $h \in \mathbb{N}^+$ denotes the number of decentralized actuator failures and may be infinite. $\sigma_{i,j,h} \in [0,1]$ is the unknown actuator efficiency factor, and $\overline{u}_{i,j,h}$ is an unknown constant indicating stuck fault in the (i,j)th actuator. The start and end of the hth failure on the (i,j)th actuator are labeled as $T^s_{i,j,h}$ and $T^e_{i,j,h}$, respectively. If $T^s_{i,j,h+1} > T^e_{i,j,h}$, a failed actuator will operate normally again during $[T^e_{i,j,h}, T^s_{i,j,h+1})$. If $T^s_{i,j,h+1} = T^e_{i,j,h}$, the failure $\sigma_{i,j,h}$ or $\overline{u}_{i,j,h}$ changes to a new one, i.e., $\sigma_{i,j,h+1}$ or $\overline{u}_{i,j,h+1}$ at time $T^e_{i,j,h}$ (or $T^s_{i,j,h+1}$). Eq. (22) implies the following three uncrossed cases:

(1) $\sigma_{i,j,h} \in (0,1)$ and $\overline{u}_{i,j,h} = 0$. In this case, $u_{i,j}(t) = \sigma_{i,j,h} v_{i,j}(t)$, which indicates partial loss of effectiveness (PLOE).

(2) $\sigma_{i,j,h} = 0$. It indicates that $u_{i,j}(t)$ can be no longer decided by the control signal $v_{i,j}(t)$. This means $u_{i,j}(t)$ is stuck at an unknown constant $\overline{u}_{i,j,h}$ (including $\overline{u}_{i,j,h} = 0$), which indicates total loss of effectiveness (TLOE).

(3) $\sigma_{i,j,h} = 1$ and $\overline{u}_{i,j,h} = 0$. In this case, the actuator works without failure.

Remark 3. Compared with the failure models in [21,23,32], the failure types in (20) and (21) are more general, because h could be infinite. In other words, some actuators can fail and recover alternately or change among different failure types infinite times if the time intervals are long enough.

Assumption 1. If the kinetic and potential energies of the flexible parts are bounded for $\forall t \geqslant 0$, then $\frac{\partial^i y(x,t)}{\partial t^i}$ or $\frac{\partial^i z(x,t)}{\partial t^i}$ is supposed to be bounded, uniformly in t for $\forall x \in [0, L)$ with $i = 1,2,3$, and $\frac{\partial^i y(x,t)}{\partial x^i}$ or $\frac{\partial^i z(x,t)}{\partial x^i}$ is supposed to be bounded, uniformly in x for $\forall t \geqslant 0$ with $i = 2,3,4$.

Assumption 2. In the presence of any TLOE type failures in up to $m_i - 1$ actuators, the system can still achieve control objectives with the remaining actuators.

Assumption 3. For the PLOE type failures, there exist unknown constants $\overline{\sigma}_{i,j}$ satisfying the condition $\sigma_{i,j,h} \geqslant \overline{\sigma}_{i,j} > 0$.

Assumption 4. The unknown disturbances d_i ($i = 1,2,3$) are assumed to vary slowly with respect to their estimation laws so that $\dot{d}_i = 0$.

Remark 4. Assumption 1 is important for system (14)–(16) to be internally stable and is deduced from an engineering point of view, commonly adopted in PDE-based analyses [32,40,41]. Assumption 2 is a condition of actuator redundancy of the system, and is a basic assumption to ensure the existence of a nominal solution for the actuator failure compensation problem [23,24]. In Assumption 3, $\overline{\sigma}_{i,j}$ is the lower bound of the actuator with PLOE type failures, which is utilized to guarantee the controllability of the system and is commonly used in a majority of existing studies [32,42,43].

Lemma 1 ([44]). Let $p(x,t)$, $q(x,t) \in \mathbb{R}$ be functions defined on $x \in [0,L]$ and $t \in [0,+\infty)$. Then the following inequality holds:

$$p(x,t)q(x,t) \leqslant \frac{1}{\gamma}p^2(x,t) + \gamma q^2(x,t), \quad \forall \gamma > 0. \tag{23}$$

Lemma 2 ([42]). For any scalars $\epsilon > 0$ and $z \in \mathbb{R}$, the following inequality holds:

$$0 \leqslant |z| - \frac{z^2}{\sqrt{z^2+\epsilon^2}} < \epsilon. \tag{24}$$

Lemma 3 ([10]). For any scalar function $z \in \mathcal{H}^1(0,L)$ with $z(0) = 0$ or $z(L) = 0$, we have

$$\int_0^L z^2(x)\mathrm{d}x \leqslant 4L^2\pi^{-2}\int_0^L z_x^2(x)\mathrm{d}x. \tag{25}$$

Moreover, if $z \in \mathcal{H}^2(0,L)$ with $z_x(0) = 0$ or $z_x(L) = 0$, then

$$\int_0^L z_x^2(x)\mathrm{d}x \leqslant 4L^2\pi^{-2}\int_0^L z_{xx}^2(x)\mathrm{d}x. \tag{26}$$

The control objective in this paper is to design a controller to stabilize the flexible spacecraft, i.e., $\lim_{t\to+\infty}\omega = 0$ and $\lim_{t\to+\infty} y(x,t) = \lim_{t\to+\infty} z(x,t) = 0$ in the presence of actuator failures and input disturbances.

3 Adaptive controller design for failure compensation

In this section, the controller will be designed relying on a Lyapunov direct method such that the attitude and the vibrations can be stabilized.

Firstly, substituting (20) into (19) yields

$$\tau_i = \sum_{j=1}^{m_i}\varrho_{i,j}u_{i,j} = \sum_{j=1}^{m_i}\varrho_{i,j}\sigma_{i,j}(t)v_{i,j}(t) + \sum_{j=1}^{m_i}\varrho_{i,j}\overline{u}_{i,j}(t). \tag{27}$$

We then have

$$\tau_i = \sum_{j=1}^{m_i}\varrho_{i,j}\sigma_{i,j}(t)v_{i,j}(t) + \delta_i^{\mathrm{T}}(t)I_{m_i}, \tag{28}$$

where $\delta_i(t) = [\varrho_{i,1}\overline{u}_{i,1}(t),\ldots,\varrho_{i,m_i}\overline{u}_{i,m_i}(t)]^{\mathrm{T}} \in \mathbb{R}^{m_i}$ and $I_{m_i} = [1,\ldots,1]^{\mathrm{T}} \in \mathbb{R}^{m_i}$.

From Assumption 3, it can be seen that $\sum_{j=1}^{m_i}|\varrho_{i,j}|\,\sigma_{i,j}(t) \geqslant \min\{|\varrho_{i,1}|\,\overline{\sigma}_{i,1},\ldots,|\varrho_{i,m_i}|\,\overline{\sigma}_{i,m_i}\} > 0$ and $\delta_i(t)$ is bounded for all $t \geqslant 0$. We further have $\inf_{t\geqslant 0}\sum_{j=1}^{m_i}|\varrho_{i,j}|\,\sigma_{i,j}(t) > 0$.

To deal with unknown actuator failures, we define the following variables:

$$l_i = \inf_{t\geqslant 0}\sum_{j=1}^{m_i}|\varrho_{i,j}|\,\sigma_{i,j}(t), \quad p_i = \frac{1}{l_i}, \quad g_i = \sup_{t\geqslant 0}\|\delta_i(t)\|, \tag{29}$$

where p_i contains both information of actuator efficiency factor $\varrho_{i,j}$ and $\sigma_{i,j}(t)$, and g_i includes the information of $\varrho_{i,j}$ and stuck fault $\overline{u}_{i,j}(t)$. We introduce a smooth, bounded, and strictly positive auxiliary signal $\zeta_i(t)$ which satisfies the following condition:

$$\int_0^{+\infty}\zeta_i(t)\mathrm{d}t < +\infty. \tag{30}$$

In this study, $\zeta_i(t)$ is chosen as $\zeta_i(t) = \sigma_{\zeta_i}\mathrm{e}^{-\lambda_{\zeta_i}t}$ with σ_{ζ_i} and λ_{ζ_i} being positive constants.

it follows from Lemma 2 and (29) that

$$\omega_i\delta_i^{\mathrm{T}}(t)I_{m_i} \leqslant g_i\,|\omega_i|\,\|I_{m_i}\| \leqslant g_i\omega_i\xi_i + g_i\zeta_i(t), \tag{31}$$

where $\xi_i = \frac{\omega_i I_{m_i}^{\mathrm{T}} I_{m_i}}{\sqrt{\omega_i^2 I_{m_i}^{\mathrm{T}} I_{m_i} + \zeta_i^2(t)}}$.

Let $\hat{g}_i$, $\hat{p}_i$, and $\hat{d}_i$ be the estimates of g_i, p_i, and d_i, respectively. Consider a Lyapunov function

$$V_1 = E_1 + E_2 + \frac{1}{2}\sum_{i=1}^{3} l_i \gamma_{p_i}^{-1} \tilde{p}_i^2 + \frac{1}{2}\sum_{i=1}^{3} \gamma_{g_i}^{-1} \tilde{g}_i^2 + \frac{1}{2}\sum_{i=1}^{3} \gamma_{d_i}^{-1} \tilde{d}_i^2, \tag{32}$$

where γ_{p_i}, γ_{g_i}, and γ_{d_i} are positive constants, $\tilde{p}_i = \hat{p}_i - p_i$, $\tilde{g}_i = \hat{g}_i - g_i$, $\tilde{d}_i = \hat{d}_i - d_i$, and

$$E_1 = \frac{1}{2}\omega^{\mathrm{T}} I_s \omega + \frac{1}{2}\rho \int_\Omega \left[\phi \frac{\mathrm{d}r}{\mathrm{d}t}\right]^{\mathrm{T}} \left[\phi \frac{\mathrm{d}r}{\mathrm{d}t}\right] \mathrm{d}x,\ E_2 = \frac{1}{2} E I_y \int_\Omega y_{xx}^2 \mathrm{d}x + \frac{1}{2} E I_z \int_\Omega z_{xx}^2 \mathrm{d}x. \tag{33}$$

By differentiating (32) with respect to time, we have

$$\dot{V}_1 = \sum_{i=1}^{3} \omega_i (\tau_i + d_i) + \Delta_1 + \sum_{i=1}^{3} l_i \gamma_{p_i}^{-1} \tilde{p}_i \dot{\hat{p}}_i + \sum_{i=1}^{3} \gamma_{g_i}^{-1} \tilde{g}_i \dot{\hat{g}}_i + \sum_{i=1}^{3} \gamma_{d_i}^{-1} \tilde{d}_i \dot{\hat{d}}_i, \tag{34}$$

where $\Delta_1 = -\gamma_b \int_\Omega \left[\phi \frac{\mathrm{d}r}{\mathrm{d}t}\right]^{\mathrm{T}} \left[\phi \frac{\mathrm{d}r}{\mathrm{d}t}\right] \mathrm{d}x$.

By substituting (28) into (34), we obtain

$$\begin{aligned} \dot{V}_1 = {} & \sum_{i=1}^{3} \sum_{j=1}^{m_i} \omega_i \varrho_{i,j} \sigma_{i,j}(t) v_{i,j}(t) + \sum_{i=1}^{3} \omega_i d_i + \sum_{i=1}^{3} \omega_i \delta_i^{\mathrm{T}}(t) I_{m_i} + \sum_{i=1}^{3} l_i \gamma_{p_i}^{-1} \tilde{p}_i \dot{\hat{p}}_i \\ & + \sum_{i=1}^{3} \gamma_{g_i}^{-1} \tilde{g}_i \dot{\hat{g}}_i + \sum_{i=1}^{3} \gamma_{d_i}^{-1} \tilde{d}_i \dot{\hat{d}}_i + \Delta_1. \end{aligned} \tag{35}$$

Using the inequality (31) yields

$$\begin{aligned} \dot{V}_1 \leqslant {} & \sum_{i=1}^{3} \sum_{j=1}^{m_i} \omega_i \varrho_{i,j} \sigma_{i,j}(t) v_{i,j}(t) + \sum_{i=1}^{3} l_i \gamma_{p_i}^{-1} \tilde{p}_i \dot{\hat{p}}_i + \sum_{i=1}^{3} \omega_i d_i + \sum_{i=1}^{3} g_i \omega_i \xi_i + \sum_{i=1}^{3} g_i \zeta_i(t) \\ & + \sum_{i=1}^{3} \gamma_{g_i}^{-1} \tilde{g}_i \dot{\hat{g}}_i + \sum_{i=1}^{3} \gamma_{d_i}^{-1} \tilde{d}_i \dot{\hat{d}}_i + \Delta_1. \end{aligned} \tag{36}$$

We then define $\overline{\alpha}_i$ as

$$\overline{\alpha}_i = c_i \omega_i + \hat{g}_i \xi_i + \hat{d}_i. \tag{37}$$

By considering (36) and (37), we have

$$\begin{aligned} \dot{V}_1 \leqslant {} & \sum_{i=1}^{3} \sum_{j=1}^{m_i} \omega_i \varrho_{i,j} \sigma_{i,j}(t) v_{i,j}(t) + \sum_{i=1}^{3} \omega_i \overline{\alpha}_i - \sum_{i=1}^{3} c_i \omega_i^2 + \sum_{i=1}^{3} \gamma_{g_i}^{-1} \tilde{g}_i (\dot{\hat{g}}_i - \gamma_{g_i} \omega_i \xi_i) + \sum_{i=1}^{3} g_i \zeta_i(t) \\ & + \sum_{i=1}^{3} \gamma_{d_i}^{-1} \tilde{d}_i (\dot{\hat{d}}_i - \gamma_{d_i} \omega_i) + \sum_{i=1}^{3} l_i \gamma_{p_i}^{-1} \tilde{p}_i \dot{\hat{p}}_i + \Delta_1. \end{aligned} \tag{38}$$

Design a control scheme

$$v_{i,j}(t) = -\operatorname{sign}(\varrho_{i,j}) \overline{v}_i, \tag{39}$$

where $\overline{v}_i = \frac{\omega_i \hat{p}_i^2 \overline{\alpha}_i^2}{\sqrt{\omega_i^2 \hat{p}_i^2 \overline{\alpha}_i^2 + \zeta_i^2(t)}}$, with parameter update laws

$$\dot{\hat{p}}_i = \gamma_{p_i} \omega_i \overline{\alpha}_i, \quad \dot{\hat{g}}_i = \gamma_{g_i} \omega_i \xi_i, \quad \dot{\hat{d}}_i = \gamma_{d_i} \omega_i. \tag{40}$$

It is worth pointing out that the feedback signals, involved in the proposed control scheme (39) and (40), are capable to address uncertainties in unknown input disturbance d_i, actuator efficiency factor $\varrho_{i,j}$ and $\sigma_{i,j}(t)$, and stuck fault $\overline{u}_{i,j}(t)$. Thus, the designed control law can be adapted to compensate unknown input disturbances and actuator failures.

Table 1 Adaptive fault tolerant control scheme for a 3D flexible spacecraft

Plant	Description
Equations of motion	Governing equations (14) and (15) and boundary conditions (16)
Assumptions	Assumptions 1–3
Defined new variables	$l_i = \inf_{t\geqslant 0}\sum_{j=1}^{m_i}\lvert\varrho_{i,j}\rvert\,\sigma_{i,j}(t),\ p_i = \frac{1}{l_i},\ g_i = \sup_{t\geqslant 0}\lVert\delta_i(t)\rVert$
Control input	$\tau_i = \sum_{j=1}^{m_i}\varrho_{i,j}u_{i,j} = \sum_{j=1}^{m_i}\varrho_{i,j}\sigma_{i,j}(t)v_{i,j}(t) + \sum_{j=1}^{m_i}\varrho_{i,j}\overline{u}_{i,j}(t)$
Auxiliary signals	$\zeta_i(t)$ satisfying $\int_0^{+\infty}\zeta_i(t)\mathrm{d}t < +\infty$
Designed control scheme	$v_{i,j}(t) = -\operatorname{sign}(\varrho_{i,j})\,\overline{v}_i,\ \overline{v}_i = \frac{\omega_i\hat{p}_i^2\overline{\alpha}_i^2}{\sqrt{\omega_i^2\hat{p}_i^2\overline{\alpha}_i^2+\zeta_i^2(t)}}$
Parameter update laws	$\dot{\hat{p}}_i = \gamma_{p_i}\omega_i\overline{\alpha}_i,\ \dot{\hat{g}}_i = \gamma_{g_i}\omega_i\xi_i,\ \dot{\hat{d}}_i = \gamma_{d_i}\omega_i$
Design parameters	c_i (i=1,2,3), α, δ_1 and δ_2 satisfying (56) and (57)

Using Lemma 2, (29), and (39), we have

$$\begin{aligned}\sum_{i=1}^{3}\sum_{j=1}^{m_i}\omega_i\varrho_{i,j}\sigma_{i,j}(t)v_{i,j}(t) &= -\sum_{i=1}^{3}\sum_{j=1}^{m_i}\omega_i\varrho_{i,j}\sigma_{i,j}(t)\operatorname{sign}(\varrho_{i,j})\,\overline{v}_i\\ &\leqslant -\sum_{i=1}^{3}\frac{l_i\omega_i^2\hat{p}_i^2\overline{\alpha}_i^2}{\sqrt{\omega_i^2\hat{p}_i^2\overline{\alpha}_i^2+\zeta_i^2(t)}} \leqslant \sum_{i=1}^{3}l_i\zeta_i(t) - \sum_{i=1}^{3}l_i\hat{p}_i\overline{\alpha}_i\omega_i. \end{aligned}\tag{41}$$

Substituting (40) and (41) into (38) and using $l_i\tilde{p}_i - l_i\hat{p}_i = -1$ yields

$$\begin{aligned}\dot{V}_1 &\leqslant -\sum_{i=1}^{3}c_i\omega_i^2 + \sum_{i=1}^{3}l_i\zeta_i(t) - \sum_{i=1}^{3}l_i\hat{p}_i\overline{\alpha}_i\omega_i + \sum_{i=1}^{3}\omega_i\overline{\alpha}_i + \sum_{i=1}^{3}g_i\zeta_i(t) + \sum_{i=1}^{3}l_i\gamma_{p_i}^{-1}\tilde{p}_i\dot{\hat{p}}_i + \Delta_1\\ &= -\sum_{i=1}^{3}c_i\omega_i^2 + \sum_{i=1}^{3}(l_i+g_i)\,\zeta_i(t) + \Delta_1. \end{aligned}\tag{42}$$

Remark 5. The proposed control scheme is summarized in Table 1. Using the proposed control, the attitude and vibration stabilization can be ensured even if there are TLOE type of faults, and infinite number of actuator failures or faults.

Moreover, compared with the previous studies [29,30,45], the control scheme (39) and (40) is developed based on the original PDEs and can avoid the spillover problems generated by traditional truncated model-based approaches.

Remark 6. It is worth mentioning that, different from [32, 43] where the specific values of $\sigma_{i,j}$ are estimated via parameter update laws, the above design estimates the bounds of the uncertainties of failures, which makes the Lyapunov function has no jump when failures occur. Therefore, the total number of actuator faults is not restricted to be finite, and the mounted actuators are allowed to switch among the healthy case and different type failures infinite times. In contrast with [43], the reported method relies on a smooth, bounded, and strictly positive auxiliary signal $\zeta_i(t)$ to asymptotically regulate w, $y(x,t)$ and $z(x,t)$ while [43] merely ensures the uniform boundedness of the vibration. Besides, by comparison with [33], a redundant actuator case is considered via adaptive methods and without Nussbaum gain technique, which extends the applicability of adaptive methods on time-varying actuator fault-tolerant control of PDE-based systems involved redundant actuators.

4 Stability analysis

Theorem 1. Under Assumptions 1–3, we consider the system (14)–(16) subjected to various types of actuator failures and input disturbances. With the developed control scheme (39) and parameter update laws (40), the actuated system is asymptotically stable, i.e., $\lim_{t\to+\infty}\omega = 0$, $\lim_{t\to+\infty}y(x,t) = \lim_{t\to+\infty}z(x,t) = 0$.

Proof. We construct the following Lyapunov candidate function

$$V = V_1 + V_2,\tag{43}$$

where

$$V_2 = \alpha\rho \int_\Omega \left[\phi \frac{\mathrm{d}r}{\mathrm{d}t}\right]^{\mathrm{T}} [\phi s] \mathrm{d}x \tag{44}$$

with a positively adjustable constant α.

We can see that (44) satisfies the following inequality:

$$\begin{aligned} |V_2| &\leqslant \frac{\alpha\rho}{2} \int_\Omega \left[\phi \frac{\mathrm{d}r}{\mathrm{d}t}\right]^{\mathrm{T}} \left[\phi \frac{\mathrm{d}r}{\mathrm{d}t}\right] \mathrm{d}x + \frac{\alpha\rho}{2} \int_\Omega [\phi s]^{\mathrm{T}} [\phi s] \mathrm{d}x \leqslant \frac{\alpha\rho}{2} \int_\Omega M(x,t) \mathrm{d}x + \frac{\alpha\rho 16 L^4}{2\pi^4} \int_\Omega \left(y_{xx}^2 + z_{xx}^2\right) \mathrm{d}x \\ &\leqslant \alpha_1 \left(E_1 + E_2\right) \leqslant \alpha_1 V_1, \end{aligned} \tag{45}$$

where $\alpha_1 = \max[\alpha, \frac{16\alpha\rho L^4}{\pi^4 E I_y}, \frac{16\alpha\rho L^4}{\pi^4 E I_z}]$, and $M(x,t) = [\phi \frac{\mathrm{d}r}{\mathrm{d}t}]^{\mathrm{T}} [\phi \frac{\mathrm{d}r}{\mathrm{d}t}]$.

Then, we have

$$-\alpha_1 V_1 \leqslant V_2 \leqslant \alpha_1 V_1. \tag{46}$$

Choosing α_1 to satisfy $0 < \alpha_1 < 1$, and defining the following two constants:

$$\alpha_2 = 1 - \alpha_1 > 0, \quad \alpha_3 = 1 + \alpha_1 > 1, \tag{47}$$

it follows from (43) and (46) that

$$0 \leqslant \alpha_2 V_1 \leqslant V \leqslant \alpha_3 V_1. \tag{48}$$

Calculating the derivative of (43) along the trajectories of the system yields

$$\dot{V} = \dot{V}_1 + \dot{V}_2. \tag{49}$$

The second term is

$$\dot{V}_2 = \alpha\rho \int_\Omega \left[\phi \frac{\mathrm{d}^2 r}{\mathrm{d}t^2}\right]^{\mathrm{T}} [\phi s] \mathrm{d}x + \alpha\rho \int_\Omega \left[\phi \frac{\mathrm{d}r}{\mathrm{d}t}\right]^{\mathrm{T}} \left[\phi \frac{\mathrm{d}s}{\mathrm{d}t}\right] \mathrm{d}x. \tag{50}$$

Simplifying the first term of (50) by integration by parts and utilizing the boundary conditions and Lemma 3 yields

$$\begin{aligned} \alpha\rho \int_\Omega \left[\phi \frac{\mathrm{d}^2 r}{\mathrm{d}t^2}\right]^{\mathrm{T}} [\phi s] \mathrm{d}x \leqslant \frac{\alpha\gamma_b}{2\delta_1} \int_\Omega M(x,t) \mathrm{d}x - \left(\alpha E I_y - \frac{\alpha\gamma_b\delta_1 16 L^4}{2\pi^4}\right) \int_\Omega y_{xx}^2 \mathrm{d}x \\ - \left(\alpha E I_z - \frac{\alpha\gamma_b\delta_1 16 L^4}{2\pi^4}\right) \int_\Omega z_{xx}^2 \mathrm{d}x. \end{aligned} \tag{51}$$

Similarly, the second term of (50) becomes

$$\alpha\rho \int_\Omega \left[\phi \frac{\mathrm{d}r}{\mathrm{d}t}\right]^{\mathrm{T}} \left[\phi \frac{\mathrm{d}s}{\mathrm{d}t}\right] \mathrm{d}x \leqslant \left(\frac{\alpha\rho\delta_2}{2} + \alpha\rho\right) \int_\Omega \left[\phi \frac{\mathrm{d}r}{\mathrm{d}t}\right]^{\mathrm{T}} \left[\phi \frac{\mathrm{d}r}{\mathrm{d}t}\right] \mathrm{d}x + \frac{\alpha\rho L^3}{6\delta_2} \left(\omega_2^2 + \omega_3^2\right), \tag{52}$$

where δ_1 and δ_2 are positive constants.

Substituting (51) and (52) into (50) yields

$$\begin{aligned} \dot{V}_2 \leqslant \left(\frac{\alpha\gamma_b}{2\delta_1} + \frac{\alpha\rho\delta_2}{2} + \alpha\rho\right) \int_\Omega M(x,t) \mathrm{d}x + \frac{\alpha\rho L^3}{6\delta_2} \left(\omega_2^2 + \omega_3^2\right) \\ - \left(\alpha E I_y - \frac{\alpha\gamma_b\delta_1 16 L^4}{2\pi^4}\right) \int_\Omega y_{xx}^2 \mathrm{d}x - \left(\alpha E I_z - \frac{\alpha\gamma_b\delta_1 16 L^4}{2\pi^4}\right) \int_\Omega z_{xx}^2 \mathrm{d}x. \end{aligned} \tag{53}$$

By substituting (42) and (53) into (49), we obtain

$$\dot{V} \leqslant -c_1\omega_1^2 - \sum_{i=2}^{3} \left(c_i - \frac{\alpha\rho L^3}{6\delta_2}\right) \omega_i^2 + \Delta + \sum_{i=1}^{3} \left(l_i + g_i\right) \zeta_i(t), \tag{54}$$

where

$$\Delta = -\left(\gamma_b - \frac{\alpha\gamma_b}{2\delta_1} - \frac{\alpha\rho\delta_2}{2} - \alpha\rho\right) \int_\Omega M(x,t) \mathrm{d}x - \left(\alpha E I_y - \frac{\alpha\gamma_b\delta_1 16 L^4}{2\pi^4}\right) \int_\Omega y_{xx}^2 \mathrm{d}x$$

$$-\left(\alpha EI_z-\frac{\alpha\gamma_b\delta_1 16L^4}{2\pi^4}\right)\int_\Omega z_{xx}^2\mathrm{d}x. \tag{55}$$

We design parameters c_i $(i=1,2,3)$, α, δ_1, and δ_2 to satisfy the following inequalities:

$$\gamma_1=c_1>0,\ \gamma_i=c_i-\frac{\alpha\rho L^3}{6\delta_2}>0,\ (i=2,3),\ \gamma_4=\gamma_b-\frac{\alpha\gamma_b}{2\delta_1}-\frac{\alpha\rho\delta_2}{2}-\alpha\rho>0, \tag{56}$$

$$\gamma_5=\alpha EI_y-\frac{\alpha\gamma_b\delta_1 16L^4}{2\pi^4}>0,\ \gamma_6=\alpha EI_z-\frac{\alpha\gamma_b\delta_1 16L^4}{2\pi^4}>0. \tag{57}$$

Then, (54) becomes

$$\dot V\leqslant-\sum_{i=1}^3\gamma_i\omega_i^2+\Delta+\sum_{i=1}^3\left(l_i+g_i\right)\zeta_i(t). \tag{58}$$

We further obtain

$$\dot V\leqslant-\lambda_1\left(E_1+E_2\right)+\sum_{i=1}^3\left(l_i+g_i\right)\zeta_i(t), \tag{59}$$

where $\lambda_1=\min[\frac{2\min(\gamma_1,\gamma_2,\gamma_3)}{\lambda_{\max}(I_s)},\frac{2\gamma_4}{\rho},\frac{2\gamma_5}{EI_y},\frac{2\gamma_6}{EI_z}]$.

Integrating both sides of (59) yields

$$V(t)-V(0)\leqslant-\lambda_1\int_0^t\left(E_1+E_2\right)\mathrm{d}\upsilon+\sum_{i=1}^3\int_0^t\left(l_i+g_i\right)\zeta_i(\upsilon)\mathrm{d}\upsilon. \tag{60}$$

According to (30), we can see $\sum_{i=1}^3\int_0^{+\infty}(l_i+g_i)\zeta_i(\upsilon)\mathrm{d}\upsilon<+\infty$. From (60), it is clear that $E_1\in\mathcal{L}_\infty$, $E_2\in\mathcal{L}_\infty$, $V\in\mathcal{L}_\infty$, and $\hat p_i$, $\hat g_i$, $\hat d_i$ for $i=1,2,3$ are bounded. Using (37), we can see that $\overline{\alpha}_i$ is bounded. Then according to (20) and (39), we can prove that the control inputs $u_{i,j}(t)$ $(j=1,\ldots,m_i)$ are bounded. Then we can conclude that all signals of the closed-loop system are globally uniformly bounded. Then based on Assumption 1 and above analysis, we can obtain that $\dot E_1\in\mathcal{L}_\infty$ and $\dot E_2\in\mathcal{L}_\infty$. Then Lemma A.6 in [40] is used to shown that $\lim_{t\to+\infty}E_1=0$ and $\lim_{t\to+\infty}E_2=0$. Using Lemma A.12 in [40], the following inequalities can be developed:

$$E_1\geqslant\frac{1}{2}\lambda_{\min}\left(I_s\right)\|\omega\|^2\geqslant0, \tag{61}$$

$$E_2\geqslant\frac{1}{2L^3}EI_y y^2(x,t)+\frac{1}{2L^3}EI_z z^2(x,t)\geqslant0. \tag{62}$$

Since $E_1\to0$ and $E_2\to0$ as $t\to+\infty$, we can conclude that $\omega\to0$, $y(x,t)\to0$ and $z(x,t)\to0$ as $t\to+\infty$, for $\forall x\in[0,L]$. This completes the proof.

Remark 7. Consider the proposed control scheme (39) and (40), the adjustable parameters include c_i, γ_{p_i}, γ_{g_i}, γ_{d_i}, and $\zeta_i(t)$ determined by σ_{ζ_i} and λ_{ζ_i}. According to (40), increasing γ_{p_i}, γ_{g_i}, and γ_{d_i} are able to speed up the updates of estimated parameters. From (59), the closed-loop performance can be optimized by increasing c_i and λ_{ζ_i}, and decreasing σ_{ζ_i} to accelerate the decay of Lyapunov function V. However, improper values may cause the instability of the resulted system. Thus, appropriate values are required to regulate the performance and simultaneously stabilize the system. Other parameters, involving α, δ_1, and δ_2, are chosen to satisfy (56) and (57), which are independent of the reported control laws (39) and (40).

Remark 8. Different from observer design in [9], the developed parameter update laws (40) resort to adaptive technique and cannot asymptotically regulate the estimations to the real values due to the asymptotical result just in the sense of $\omega(t)$, $y(x,t)$, and $z(x,t)$ in Theorem 1, which means the estimations may be convergent to some irrelevant values.

5 Numerical simulation

In this study, the finite difference method is utilized to conduct the numerical simulations. For simplification of the analysis, we assume that the satellite body inertia matrix is diagonal. The parameters of

the 3D flexible spacecraft are listed in Table 2. According to Assumption 4, the proposed adaptive robust control method is capable to address a perturbation with lower rate. To be close to theoretical analysis, the input disturbances with constant values are given as

$$\begin{cases} d_1(t) = 2\ \mathrm{N}\cdot\mathrm{ft}, \\ d_2(t) = 1\ \mathrm{N}\cdot\mathrm{ft}, \\ d_3(t) = 6\ \mathrm{N}\cdot\mathrm{ft}. \end{cases} \tag{63}$$

The initial conditions are given as follows:

$$\begin{cases} \omega_1(0) = 0.02\ \mathrm{rad/s}, \\ \omega_2(0) = 0.03\ \mathrm{rad/s}, \\ \omega_3(0) = 0.04\ \mathrm{rad/s}, \end{cases} \quad \text{and} \quad \begin{cases} y(x,0) = z(x,0) = 0.1x/L,\ x \in \Omega, \\ \dot{y}(x,0) = \dot{z}(x,0) = 0,\ x \in \Omega. \end{cases} \tag{64}$$

To facilitate the subsequence numerical simulations, we set

$$\begin{cases} \tau_1(t) = u_{1,1}(t) + u_{1,2}(t), \\ \tau_2(t) = u_{2,1}(t) + u_{2,2}(t), \\ \tau_3(t) = u_{3,1}(t) + u_{3,2}(t). \end{cases} \tag{65}$$

Besides, the unknown failures of the actuators are set as

$$\begin{cases} u_{1,1}(t) = v_{1,1}(t),\ u_{1,2}(t) = 0.3v_{1,2}(t),\ u_{2,1}(t) = v_{2,1}(t),\ u_{2,2}(t) = v_{2,2}(t),\ u_{3,1}(t) = v_{3,1}(t), \\ \qquad \text{if } t \in [2k, 2k+1), \\ u_{1,1}(t) = 0.5v_{1,1}(t),\ u_{1,2}(t) = 0,\ u_{2,1}(t) = 0,\ u_{2,2}(t) = v_{2,2}(t),\ u_{3,1}(t) = 0.6v_{3,1}(t), \\ \qquad \text{if } t \in [2k+1, 2k+2), \end{cases} \tag{66}$$

$$\text{and } u_{3,2}(t) = \begin{cases} v_{3,2}(t), & \text{if } t \in [0, 6), \\ u_{3,2}(6), & \text{if } t \in [6, +\infty), \end{cases}$$

where $k = 0, 1, 2, \ldots$. From (66) we can see that during every time interval $[2k, 2k+1)$, the actuators $u_{1,1}$, $u_{2,1}$, and $u_{3,1}$ operate normally, but the actuator $u_{1,2}$ loses 70% of its effectiveness. While during the interval $[2k+1, 2k+2)$, the actuators $u_{1,1}$, $u_{1,2}$, $u_{2,1}$, and $u_{3,1}$ lose 50%, 100%, 100%, and 40% of their effectiveness, respectively. $u_{2,2}$ operates normally during arbitrary time interval and $u_{3,2}$ fails completely after $t = 6$ s.

Because there is seldom literature on how to control the attitude and the vibrations of the 3D PDE model simultaneously, PD control laws are adopted to demonstrate the effectiveness of the proposed control scheme (39) and (40).

The PD control laws are designed as follows:

$$v_{i,j}(t) = -k_{pi}\omega_i(t) - k_{di}\dot{\omega}_i(t), \tag{67}$$

where $i = 1, 2, 3$, $j = 1, 2$.

In the control design, the designed parameters are chosen as $c_i = 15$, $\gamma_{p_i} = 18$ and $\gamma_{g_i} = \gamma_{d_i} = 10$, and the auxiliary signals $\zeta_i(t)$ are given by $\zeta_i(t) = 0.5\mathrm{e}^{-0.4t}$, where $i = 1, 2, 3$. The PD control gains are set as $k_{p1} = 100$, and $k_{d1} = k_{p2} = k_{d2} = k_{p3} = k_{d3} = 50$.

The simulation results are shown in Figures 3–10. Figures 3–5 illustrate the effectiveness of the proposed control strategy (39) in stabilizing the flexible spacecraft, even in the cases where the repeated unknown failures occur on the actuators. Besides, we can see that all signals of the actuated system are bounded and tend to zero asymptotically. Compared with the proposed control laws, an integrally disabled performance generated by PD controllers is depicted by Figures 3 and 4, due to the dynamic coupling among three dimensions and perturbation from failed actuators and input disturbances. Figures 6–8 show that all the parameter estimations are bounded with the employed parameter update laws (40). The output signal of the (i, j)th ($i = 1, 2, 3$; $j = 1, 2$) actuator and the control torque at the spherical driving devices in the presence of the different types of actuator failures are depicted in Figures 9 and 10, respectively. Figure 9 shows that the amplitude of the control torque is reduced at the time instants when PLOE occurs and remains unchanged at the time instants when TLOE in actuator takes place. However, the control torque stays within a reasonable scope in all cases, and all states are regulated well within 12 s.

Table 2 Parameters of a 3D flexible spacecraft

Parameter	Description	Value
L	The length of the panel	18.8 ft
EI_y	The flexural rigidity of the panel in OY_b axis	3550.8 lb·ft^2
EI_z	The flexural rigidity of the panel in OZ_b axis	3550.8 lb·ft^2
I_{s1}	The inertia tensor of the rigid satellite in OX_o axis	645 slug·ft^2
I_{s2}	The inertia tensor of the rigid satellite in OY_o axis	100 slug·ft^2
I_{s3}	The inertia tensor of the rigid satellite in OZ_o axis	669 slug·ft^2
ρ	The mass density of the panel	2.86e-2 slug/ft
γ_b	Panel damping	0.01 N·s/ft

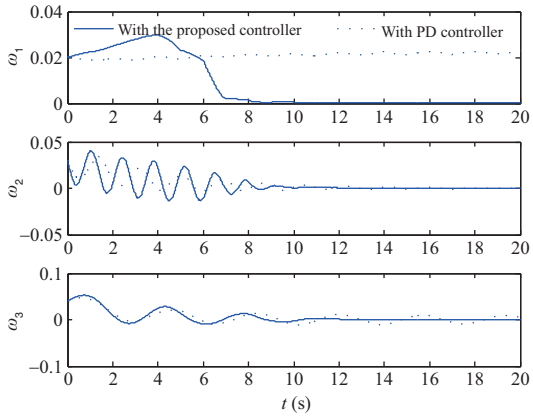

Figure 3 (Color online) Satellite angular velocities ω_i (rad/s), $i = 1, 2, 3$.

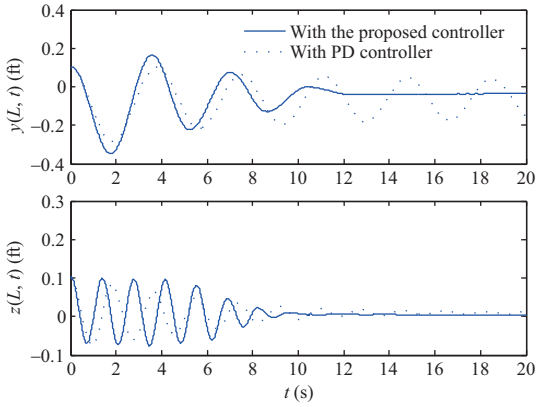

Figure 4 (Color online) Displacements of the panel's free point along the Y_b and Z_b axes.

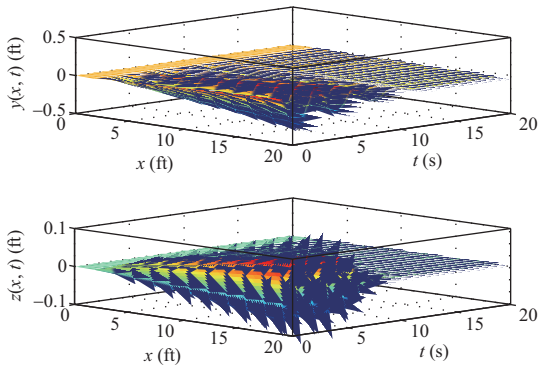

Figure 5 (Color online) Deflection evolution profiles of the spacecraft along the Y_b and Z_b axes with the proposed controllers.

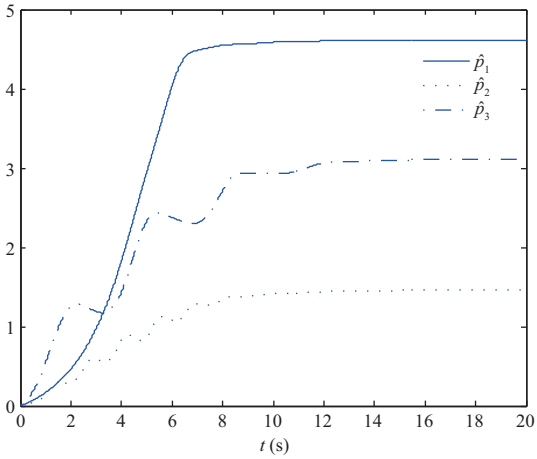

Figure 6 (Color online) Parameter estimations for p_i ($i = 1, 2, 3$).

6 Conclusion

This paper presented the modeling and simultaneous attitude and vibration control of the flexible spacecraft in a 3D space under input disturbances and unknown actuator failures. The system is described by coupled PDEs and ODEs. When the panel deflections are zero, the system can be described as a well-known dynamic model of a rigid spacecraft. Moreover, if the coupling of the deflections along the Y_b and Z_b axes is not considered, the system can reduce to the common equations for flexible spacecraft in a 2D space. The reported control solution guarantees asymptotic regulation of the attitude and suppression of the distributed deflections, even in the case of a possibly infinite number of unknown actuator fail-

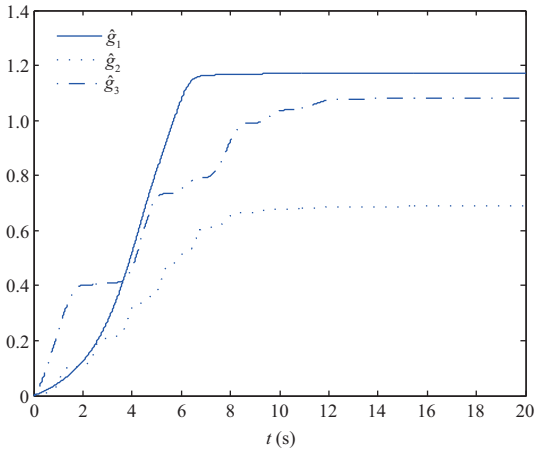

Figure 7 (Color online) Parameter estimations for g_i $(i = 1, 2, 3)$.

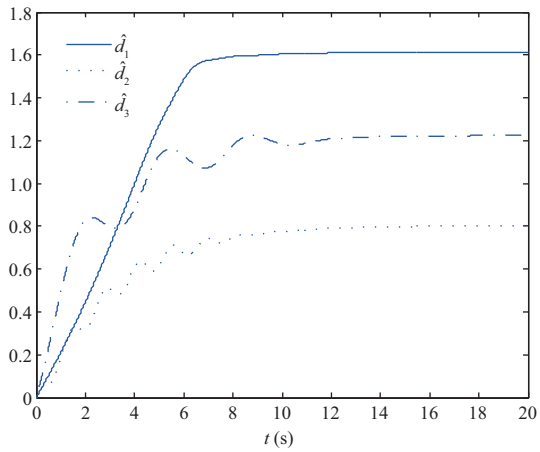

Figure 8 (Color online) Parameter estimations for d_i $(i = 1, 2, 3)$.

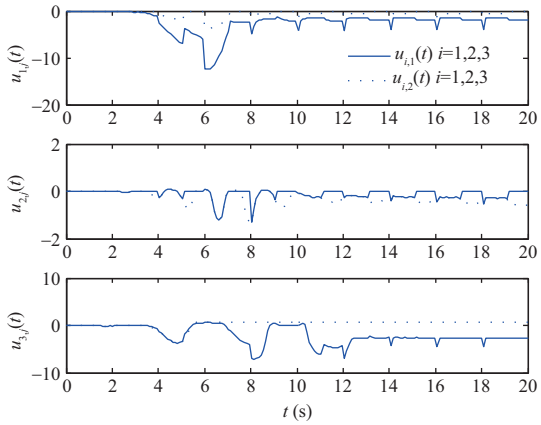

Figure 9 (Color online) The actual torque $u_{i,j}$ (N · ft), $i = 1, 2, 3$, $j = 1, 2$ generated by a single actuator.

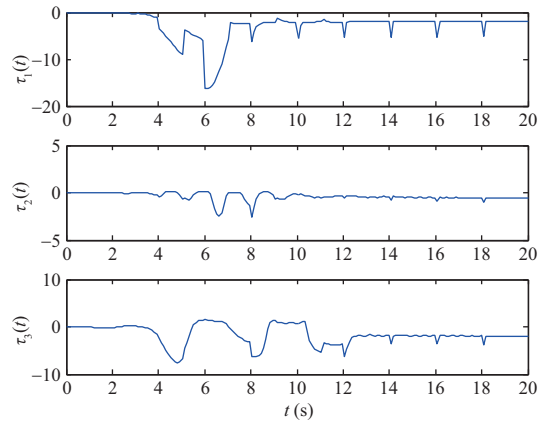

Figure 10 (Color online) The control torque τ_i (N · ft), $i = 1, 2, 3$ at the spherical driving joints.

ures and input disturbances. The proposed control method can be applied to the time-varying actuator fault-tolerant control of PDE-based systems, which are involved in redundant actuators. In future work, we will use an intelligent control method [46–49] to design the attitude tracking and vibration control scheme for flexible spacecraft based on PDEs.

Acknowledgements This work was supported by National Natural Science Foundation of China (Grant No. 62073030), Interdisciplinary Research Project for Young Teachers of USTB (Grant No. FRF-IDRY-19-024), Guangdong Basic and Applied Basic Research Foundation (Grant No. 2019A1515110728), Postdoctor Research Foundation of Shunde Graduate School of University of Science and Technology Beijing (Grant No. 2020BH002), and Beijing Top Discipline for Artificial Intelligent Science and Engineering, University of Science and Technology Beijing.

References

1 Gennaro S D. Output stabilization of flexible spacecraft with active vibration suppression. IEEE Trans Aerosp Electron Syst, 2003, 39: 747–759

2 Hu Q L, Ma G F. Variable structure control and active vibration suppression of flexible spacecraft during attitude maneuver. Aerospace Sci Tech, 2005, 9: 307–317

3 Hu Q. Adaptive output feedback sliding-mode manoeuvring and vibration control of flexible spacecraft with input saturation. IET Control Theory Appl, 2008, 2: 467–478

4 Liu H, Guo L, Zhang Y M. An anti-disturbance PD control scheme for attitude control and stabilization of flexible spacecrafts. Nonlinear Dyn, 2012, 67: 2081–2088

5 Chen T, Wen H, Wei Z T. Distributed attitude tracking for multiple flexible spacecraft described by partial differential equations. Acta Astronaut, 2019, 159: 637–645

6 He W, Ge S S. Dynamic modeling and vibration control of a flexible satellite. IEEE Trans Aerosp Electron Syst, 2015, 51: 1422–1431

7 Ji N, Liu J K. Vibration control for a flexible satellite with input constraint based on Nussbaum function via backstepping method. Aerospace Sci Tech, 2018, 77: 563–572

8 Feng S, Wu H N. Hybrid robust boundary and fuzzy control for disturbance attenuation of nonlinear coupled ODE-beam systems with application to a flexible spacecraft. IEEE Trans Fuzzy Syst, 2017, 25: 1293–1305

9 Liu Y, Fu Y, He W, et al. Modeling and observer-based vibration control of a flexible spacecraft with external disturbances. IEEE Trans Ind Electron, 2019, 66: 8648–8658

10 Wang J W, Liu Y Q, Sun C Y. Observer-based dynamic local piecewise control of a linear parabolic PDE using non-collocated local piecewise observation. IET Control Theory Appl, 2018, 12: 346–358

11 Wang J, Krstic M. Output feedback boundary control of a heat PDE sandwiched between two ODEs. IEEE Trans Autom Control, 2019, 64: 4653–4660

12 He W, Meng T T, He X Y, et al. Iterative learning control for a flapping wing micro aerial vehicle under distributed disturbances. IEEE Trans Cybern, 2019, 49: 1524–1535

13 Zhao Z J, He X Y, Ren Z G, et al. Boundary adaptive robust control of a flexible riser system with input nonlinearities. IEEE Trans Syst Man Cybern Syst, 2019, 49: 1971–1980

14 Zhao Z J, Ahn C K, Li H X. Dead zone compensation and adaptive vibration control of uncertain spatial flexible riser systems. IEEE/ASME Trans Mechatron, 2020, 25: 1398–1408

15 Ren Y, Chen M, Liu J Y. Bilateral coordinate boundary adaptive control for a helicopter lifting system with backlash-like hysteresis. Sci China Inf Sci, 2020, 63: 119203

16 Zhao Z J, Ahn C K, Li H X. Boundary antidisturbance control of a spatially nonlinear flexible string system. IEEE Trans Ind Electron, 2020, 67: 4846–4856

17 Liu Z J, Zhao Z J, Ahn C K. Boundary constrained control of flexible string systems subject to disturbances. IEEE Trans Circ Syst II, 2020, 67: 112–116

18 He W, Ge S S, Huang D Q. Modeling and vibration control for a nonlinear moving string with output constraint. IEEE/ASME Trans Mechatron, 2015, 20: 1886–1897

19 Do K D, Pan J. Boundary control of three-dimensional inextensible marine risers. J Sound Vib, 2009, 327: 299–321

20 Do K D, Lucey A D. Stochastic stabilization of slender beams in space: modeling and boundary control. Automatica, 2018, 91: 279–293

21 Tao G, Chen S, Joshi S M. An adaptive actuator failure compensation controller using output feedback. IEEE Trans Autom Control, 2002, 47: 506–511

22 Wang W, Wen C Y. Adaptive actuator failure compensation control of uncertain nonlinear systems with guaranteed transient performance. Automatica, 2010, 46: 2082–2091

23 Cai J P, Wen C Y, Su H Y, et al. Robust adaptive failure compensation of hysteretic actuators for a class of uncertain nonlinear systems. IEEE Trans Autom Control, 2013, 58: 2388–2394

24 Wang W, Wen C Y. Adaptive compensation for infinite number of actuator failures or faults. Automatica, 2011, 47: 2197–2210

25 Wang C L, Wen C Y, Lin Y. Adaptive actuator failure compensation for a class of nonlinear systems with unknown control direction. IEEE Trans Autom Control, 2017, 62: 385–392

26 Lin H W, Zhao B, Liu D R, et al. Data-based fault tolerant control for affine nonlinear systems through particle swarm optimized neural networks. IEEE/CAA J Autom Sin, 2020, 7: 954–964

27 Xiao B, Hu Q L, Shi P. Attitude stabilization of spacecrafts under actuator saturation and partial loss of control effectiveness. IEEE Trans Contr Syst Technol, 2013, 21: 2251–2263

28 Zhang A H, Hu Q L, Zhang Y M. Observer-based attitude control for satellite under actuator fault. J Guid Control Dyn, 2015, 38: 806–811

29 Ma Y J, Jiang B, Tao G, et al. Uncertainty decomposition-based fault-tolerant adaptive control of flexible spacecraft. IEEE Trans Aerosp Electron Syst, 2015, 51: 1053–1068

30 Sun G H, Xu S D, Li Z. Finite-time fuzzy sampled-data control for nonlinear flexible spacecraft with stochastic actuator failures. IEEE Trans Ind Electron, 2017, 64: 3851–3861

31 Hu Q L, Xiao B. Fault-tolerant sliding mode attitude control for flexible spacecraft under loss of actuator effectiveness. Nonlinear Dyn, 2011, 64: 13–23

32 Liu Z J, Liu J K, He W. Robust adaptive fault tolerant control for a linear cascaded ODE-beam system. Automatica, 2018, 98: 42–50

33 Xing X Y, Liu J K. PDE modelling and vibration control of overhead crane bridge with unknown control directions and parametric uncertainties. IET Control Theory Appl, 2020, 14: 116–126

34 Krstic M, Smyshlyaev A. Adaptive control of PDEs. Annu Rev Control, 2008, 32: 149–160

35 Krstic M, Smyshlyaev A. Adaptive boundary control for unstable parabolic PDEs-part I: Lyapunov design. IEEE Trans Autom Control, 2008, 53: 1575–1591

36 Roman C, Bresch-Pietri D, Prieur C, et al. Robustness to in-domain viscous damping of a collocated boundary adaptive

feedback law for an antidamped boundary wave PDE. IEEE Trans Autom Control, 2019, 64: 3284–3299
37 Anfinsen H, Aamo O M. Adaptive control of linear 2×2 hyperbolic systems. Automatica, 2018, 87: 69–82
38 Wang J, Tang S X, Krstic M. Adaptive output-feedback control of torsional vibration in off-shore rotary oil drilling systems. Automatica, 2020, 111: 108640
39 Wang J, Tang S X, Pi Y J, et al. Exponential regulation of the anti-collocatedly disturbed cage in a wave PDE-modeled ascending cable elevator. Automatica, 2018, 95: 122–136
40 de Queiroz M S, Dawson D M, Nagarkatti S P, et al. Lyapunov-Based Control of Mechanical Systems. New York: Springer Science + Business Media, 2012
41 Bialy B J, Chakraborty I, Cekic S C, et al. Adaptive boundary control of store induced oscillations in a flexible aircraft wing. Automatica, 2016, 70: 230–238
42 Wang C L, Wen C Y, Lin Y. Decentralized adaptive backstepping control for a class of interconnected nonlinear systems with unknown actuator failures. J Franklin Inst, 2015, 352: 835–850
43 Ji N, Liu J K. Adaptive actuator fault-tolerant control for a three-dimensional Euler-Bernoulli beam with output constraints and uncertain end load. J Franklin Inst, 2019, 356: 3869–3898
44 Rahn C D. Mechatronic Control of Distributed Noise and Vibration. Berlin: Springer, 2001
45 Xiao B, Hu Q L, Zhang Y M. Fault-tolerant attitude control for flexible spacecraft without angular velocity magnitude measurement. J Guid Control Dyn, 2011, 34: 1556–1561
46 Xie G, Shangguan A Q, Fei R, et al. Motion trajectory prediction based on a CNN-LSTM sequential model. Sci China Inf Sci, 2020, 63: 212207
47 Liu L, Liu Y J, Li D P, et al. Barrier Lyapunov function-based adaptive fuzzy FTC for switched systems and its applications to resistance-inductance-capacitance circuit system. IEEE Trans Cybern, 2020, 50: 3491–3502
48 Zhou T L, Chen M, Yang C G, et al. Data fusion using Bayesian theory and reinforcement learning method. Sci China Inf Sci, 2020, 63: 170209
49 Yu X B, He W, Li Y N, et al. Adaptive NN impedance control for an SEA-driven robot. Sci China Inf Sci, 2020, 63: 159207